WCAP-16996-P, "Realistic LOCA Evaluation Methodology Applied to the Full Spectrum of Break Sizes (FULL SPECTRUM LOCA Methodology)" Requests for Additional Information – Third Set (Non-Proprietary)

May 2013

Westinghouse Electric Company LLC
1000 Westinghouse Drive
Cranberry Township, PA 16066

RAI #30 – Scaling of the Westinghouse Vertical COSI Test Facility and Tests

WCAP-16996-P/WCAP-16996-NP, Volumes I, II and III, Revision 0, "Realistic LOCA [Loss-of-Coolant-Accident] Evaluation Methodology Applied to the Full Spectrum of Break sizes (FULL SPECTRUM™ LOCA [(FSLOCA™)] Methodology)," Subsection 6.3.6, "Special Model: Cold Leg Condensation Model," describes the model for predicting direct contact condensation on the Safety Injection (SI) water for both small-break LOCA (SBLOCA) and large-break LOCA (LBLOCA) applications. The model employs an [ ]^{a,c} that was derived from a best fit to a set of data points derived from tests at the Westinghouse Condensation on Safety Injection (COSI) test facility. The facility is referred to as the Westinghouse vertical COSI test facility and the tests as the Westinghouse vertical COSI tests. [

]^{a,c}

[

a,c

]

WCAP-16996-P/WCAP-16996-NP, Volumes I, II and III, Revision 0, Subsection 6.3.6 states that the Westinghouse vertical COSI test facility "geometrically is a 1:100 scale of a pressurized water reactor (PWR) cold leg." Additional information on scaling of a similar test facility is provided by P. Coste et al., "Status of a Two-Phase computational fluid dynamics (CFD) Approach to the PTS Issue," Proc. OECD/NEA & IAEA Workshop "Experiments and CFD Code Applications to Nuclear Reactor Safety," September 10-12, 2008, Grenoble, France. This reference explains that "COSI represents a PWR cold leg with the safety injection at the scale of 1/100 for volume and power, and conservation of Froude number" from a PWR under SBLOCA conditions.

WCAP-16996-P/WCAP-16996-NP, Volumes I, II and III, Revision 0, Subsection 17.2.1, "Test Facilities and Tests Description," explains that a large matrix of tests was conducted over the course of the COSI program by both Westinghouse and Framatome and that "some reconfigurations of the facility test section were performed with regard to the length of the main pipe in the test assembly and the angle and size of the injection piping." Please clarify and address, as appropriate, the following items related to the scaling of the Westinghouse vertical COSI test facility and test matrix conditions used to produce the data set for fitting the FSLOCA methodology cold condensation correlation.

(1) Please describe the scaling of the Westinghouse vertical COSI test facility geometry and test matrix conditions used to produce the cold leg condensation rates. For this purpose, provide specific scaling relationships and criteria that are considered appropriate for investigation of SI cold leg condensation. Include specific consideration of cold leg diameter and cold leg length. Explain how the defined relationships and criteria apply to the Westinghouse vertical COSI test facility geometry and test matrix conditions. Explain which parameters and criteria support the scalability of the Westinghouse vertical COSI test data to prototypical conditions and which limit their applicability to such conditions.

(2) Based on the applied experimental procedures and conditions, data analysis, and scaling, describe the impact of involved major experimental distortions, test limitations, contributing processes, and uncertainties, related to the COSI test geometry and test conditions, on the applicability of the derived condensation data set to prototypical PWR conditions. In particular, please address such impacts related to the cold leg diameter scale.

Response:

The COSI test facility was intended to investigate the condensation in the cold leg caused by the high head safety injection (SI) during a small break LOCA. The test facility was designed to properly downscale the cold leg of a Westinghouse PWR, as well as the steam flow rate, and SI rate to replicate the thermal hydraulics phenomena in the PWR cold leg.

As discussed in Section 6.3.6 of WCAP-16996-P, a special cold leg condensation model was developed from a subset of the data generated from the COSI test facility, specifically the Westinghouse vertical COSI test facility. The model was then validated by an independent data set spanning of different scales.

The scaling and applicability of the cold leg condensation model is based on the following principles which will be further elaborated in this response:

1) [

2)

3)

4)

]^{a,c}

1. Geometrical Scaling

The cold leg test section of the Westinghouse COSI facility was shown in Figure 17-2 of WCAP-16996-P. The inner diameter of the cold leg pipe is 0.118m (4.65 inch) and its length is approximately 4.9 m (16ft). The prototypical cold leg inner diameter in Westinghouse PWRs is 0.7m (27.5inch). The cold leg diameter scaling factor between the COSI test facility and a PWR cold leg is 1/6,

$$\frac{D_T}{D_P} = \frac{0.118}{0.7} \cong \frac{1}{6}$$

where the subscript T refers to the COSI test facility and the subscript P refers to the prototype, which is a Westinghouse PWR. The flow area scaling factor between the COSI test facility and a PWR cold leg is thus obtained,

$$\frac{A_T}{A_P} = \left(\frac{D_T}{D_P}\right)^2 \cong \frac{1}{35}$$

The diameter of the COSI SI line attached to the cold leg is scaled based on the geometrical similarity between the cold leg and SI line. Thus, its scaling factor is the same as the cold leg.

$$\frac{(D_{SI})_T}{(D_{SI})_P} = \frac{D_T}{D_P} \cong \frac{1}{6}$$

$$\frac{(A_{SI})_T}{(A_{SI})_P} = \left(\frac{(D_{SI})_T}{(D_{SI})_P}\right)^2 \cong \frac{1}{35}$$

The diameters of a typical high head SI line, a typical charging line and an accumulator line are [ ]^{a,c}, respectively. The corresponding diameters in the COSI test facility are 0.9 inch (0.023m), 0.22 inch (0.0056m) and 1.5 inch (0.0381m), respectively. The scaling factors of those SI lines confirm the scaling factor of 1/6 (Table 1).

Table 1. Scaling Factors of SI lines Attached to Cold Leg

[ ]^{a,c}

Note that the reported volume scaling of 1/100 (Sections 6.3.6 and 17.2.1 of WCAP-16996-P) is misleading and for the purpose of the scaling analysis it is more appropriate to focus on the specific geometric components:.[ ]^{a,c}

2. Adequacy of Jet Re Number as Main Scaling Parameter

The historical path leading to the cold leg direct contact condensation model and the theoretical basis of the model are presented herein to facilitate the discussion. Asaka et al. [1] proposed a direct contact condensation model for TRAC-PF1/MOD 1 using turbulent liquid jet condensation model. Bestion and Gros d'Aillon [2] studied direct contact condensation in the cold leg with the data from the COSI test facility. They developed a mixing zone concept and assumed the vicinity of injection plays the most important role in the cold leg condensation. Janicot and Bestion [3] did further theoretical study on turbulence induced condensation in the vicinity of SI injection. A more accurate condensation model was developed by Janicot and Bestion using the COSI test data and the model was incorporated into the CATHARE reactor safety analysis code and validated against COSI experimental data [3]. A cold leg condensation model was incorporated into the Westinghouse NOTRUMP Appendix-K small break LOCA safety analysis code [12]. The NOTRUMP model also assumes the majority of condensation takes place immediately around the zone of the injection point based on findings from the COSI tests and a correlation was developed based on the assumed jet surface area. The development of a best-estimate small break LOCA evaluation model drove Westinghouse to develop a more scalable

cold leg condensation model than existing models for the FULL SPECTRUM™ LOCA (FSLOCA™) methodology. According to the surface renewal theory [4, 5, 6], the condensation heat transfer is controlled by the turbulent characteristics at the liquid side interface.

An accurate prediction on the condensation heat transfer relies on correlating liquid side heat transfer coefficient with the turbulent Reynolds number, which is shown in recent computational fluid dynamics simulations on the cold leg condensation problem [7, 8, 9]. In a coarse two fluid model, the detail of turbulent structure is beyond the resolution of the code. Instead, the SI jet Reynolds number, which is the kinetic source of the turbulence in the cold leg, becomes the controlling parameter.

The cold leg condensation correlation, which is used to predict the cold leg condensation rate in the cold leg condensation model was developed using the experiments from the Westinghouse vertical COSI test facility that represents a small break LOCA cold leg condensation scenario. Then, in the FSLOCA methodology, the cold condensation model is applied to the large break LOCA prediction. As addressed in Section 6.3.6 and Section 17.3 of WCAP-16996-P, the cold leg condensation scenario in a large break LOCA is different from that of a small break LOCA. As such, the application of the developed cold leg condensation model to large break LOCA is supported by the validation against the full scale cold leg condensation tests, UPTF 8A and UPTF 25A (Section 17.3 and Section 19.3 of WCAP-16996-P). [

]^{a,c}

The following sections discuss the effect of [

] ^{a,c}

3. Adequacy of Cold Leg Diameter Scaling

In the cold leg condensation theory in WCAP-16996-P, [

]^{a,c}

One arguable effect caused by the 1/6 scaling factor of cold leg diameter in the COSI test facility is [

]^{a,c} The effect was illustrated in Figure 6-13 of WCAP-16996-P. To demonstrate that [ ]^{a,c} when the cold leg condensation phenomenon is scaled up to a PWR cold leg, a comparison of [ ]^{a,c} in the COSI test facility and the Beaver Valley Unit 1 cold leg was conducted using a computational fluid dynamics (CFD) tool in Westinghouse. The computational domain is displayed in Figure 1. The simulated COSI case is W012-1, which is a charging line case with the minimum SI flow rate, the most challenging COSI test in term of the SI jet penetration. The SI diameter and flow rate are scaled using scaling factors of 1/6 and [ ]^{a,c}, respectively. Note, the flow rate scale is larger than the scaling factor between the COSI facility and Beaver Valley Unit 1, but that leads to an even smaller SI flow in the Beaver Valley Unit 1 CFD case, which would tend to

show a [ ]a,c The major parameters for the CFD computation are listed in Table 2. To [ ]a,c

The mesh was created by the TrueGrid mesh generation code. There are [ ]a,c cells in the COSI W012-1 CFD case and [ ]a,c cells in the Beaver Valley Unit 1 CFD case. The simulations were conducted using the Ansys CFX software.

Figure 2 shows the velocity profile at the cross section of the cold leg in the Westinghouse COSI test facility. The corresponding case in the cold leg of DLW is shown in Figure 3. In both cases, [ ]a,c

Table 2. Major Parameters Used in the CFD Study

[ ]a,c

4. Impact of Cold Leg and SI line Area Scaling on Flow Regime

The COSI facility is properly designed to [ ]a,c The [ ]a,c in all Westinghouse COSI test was supported by the flow regime study using the well-recognized Taitel-Dukler flow regime map [11]. [ ]a,c

To determine the flow regime in the COSI SI line, the Froude number scaling factor of the SI line is evaluated [ ]a,c

5. Impact of Cold Leg Length Scaling

A noticeable feature of the COSI test facility is the length of the cold leg. The scaling factor of the cold leg length between Westinghouse COSI and PWRs is [ ]^{a,c} The scaling factor is much larger than the scaling factor of the cold leg diameter. As discussed in Section 6.3.6 of WCAP-16996-P, the majority of cold leg condensation, when flow is stratified, is caused by the safety injection and occurs in the mixing zone. Outside the mixing zone, the stratification suppresses the interfacial heat transfer. [

]^{a,c} This will be further addressed in Section 5.

More evidence supporting that the condensation occurs in the mixing zone comes from the COSI tests. The temperature profile from thermocouple rakes showed similarity between the profile near the SI jet and the profile further downstream. Furthermore, Shimeck [10] indicated that the Framatome COSI test facility considered a much shorter cold leg length than the Westinghouse test facility, but comparison between the Framatome test data and the Westinghouse test data showed that a shorter cold leg only led to a moderate decrease in the condensation heat transfer rate. These points support the assumption of the majority of the condensation is in the mixing zone, and the assumption has been adopted by several existing cold leg condensation models by both Westinghouse and Framatome.

[

]^{a,c}

With respect to the validation of the cold leg condensation model, a favorable prediction of the Framatome tests (shorter cold leg) and ROSA SB-CL-05 (a better scaled cold leg length) is obtained. The validation against Framatome COSI was provided in WCAP-16996-P. In the response to RAI 33, an evaluation will be provided that shows [

]^{a,c}.

6. Impact of Jet Re Scaling

The geometry scaling was determined to maintain prototypical conditions with respect to flow regimes and SI jet to stratified cold leg impingement mechanisms as discussed in the previous sections. However, [

]^{a,c} as shown in Table 6-2 of WCAP-16996-P.

Figure 7 shows the ratio between the estimated condensation rate in the entire cold leg and measured value for the set of validation cases as a function of the SI Re number. Note that [

]^{a,c}

The analysis of the figure leads to the following observations:

1) [

2)

3)

4)

]^{a,c}

Further evidence of the [
]^{a,c} is provided in the response to RAI 33. It shows that the cold leg condensation rate predicted [
]^{a,c}

7. Summary on Scaling of COSI Facility

In summary, multiple aspects of scaling analyses on the diameter, flow area, length, superficial velocity, Reynolds number of both cold leg and SI line, and Froude number of SI line in the Westinghouse COSI test facility are provided. The scaling factor of SI jet Reynolds number and the cold leg diameter was further investigated. [

] ^{a,c}

References:

1. Asaka, H., Murao, Y., and Kukita, Y., "Assessment of TRAC-PF1 Condensation Heat Transfer Model for Analysis of ECC Water Injection Transition," Journal of Nuclear Science and Technology, 26 (11), pp. 1045-1167, 1989.
2. Bestion, D., and Gros d'Aillon, L., " Condensation Tests Analysis and Correlation for the CATHARE Code," Proceeding of 4th International Topical Meeting on Nuclear Reactor Thermal-Hydraulics, Karlsruhe, Germany, October 1989.
3. Janicot, A., and Bestion, D., "Condensation modeling for ECC injection," Nuclear Engineering and Design, Vol. 145, pp. 37-45, 1993.
4. Theofanous, T., Houze, R., and Brumfield, "Turbulent Mass Transfer at Free Gas-Liquid Interface, with Applications to Open-Channel, Bubble and Jet Flows," International Journal of Heat and Mass Transfer, 19 (9), pp. 613-624, 1976.
5. Banerjee, S., "A Surface Renewal Model for Interfacial Heat and Mass Transfer in Transient Two-Phase Flow," International Journal of Multiphase Flow Vol. 4, pp. 571-573, 1978.
6. Hughes, E.D., and Duffey, R.B., "Direct Contact Condensation and Momentum Transfer in Turbulent Separated Flows," International Journal of Multiphase Flow Vol. 17 pp. 599-619, 1991.

7. Coste, P., et al., "Status of a Two-Phase CFD Approach to the PTS Issue," Proc. OECD/NEA & IAEA Workshop "Experiments and CFD Code Applications to Nuclear Reactor Safety," 10-12 September 2008, Grenoble, France.
8. Glantz, T., "COSI Test Case Simulation with CFX Code", Proceedings of the 17th International Conference on Nuclear Engineering (ICONE17), July 12-16, 2009, Brussels, Belgium.
9. Labois, M., and Lakehal, D., "PTS Prediction Using the CMFD Code TransAT: the COSI Test Case," Computational Fluid Dynamics (CFD) for Nuclear Reactor Safety Applications Workshop Proceedings, CFD4NRS-3, Bethesda, Maryland, USA, September 14-16, 2010.
10. WCAP-11767, "COSI SI/Steam Condensation Experiment Analysis," March 1988.
11. Taitel, Y., and Dukler, A., "A Model for Predicting Flow Regime Transitions in Horizontal and Near Horizontal Gas-Liquid Flow," AIChE Journal, Vol. 22, No. 1, pp. 47-54, 1976.
12. WCAP-10054-P, Addendum 2, Revision 1, "Addendum to the Westinghouse Small Break ECCS Evaluation Model Using the NOTRUMP Code: Safety Injection into the Broken Loop and COSI Condensation model," October 1995.

a,c

Figure 1. The COSI computational domain.

a,c

Figure 2. Total velocity contour at the cross section of the cold leg in Westinghouse COSI test facility (W012, point 1).

a,c

Figure 3. Total velocity contour at the cross section of the cold leg of Beaver Valley Unit 1 (SI flow rate scale of 1/14).

a,c

Figure 4. Plot of jg and jl in the Westinghouse COSI tests (both vertical and horizontal COSI tests) at 4.2MPa against the Taitel- Dukler flow regime map. The horizontal stratified flow regime is inside the solid line.

a,c

Figure 5. Plot of jg and jl in the Westinghouse COSI tests (both vertical and horizontal COSI tests) at 5.6MPa against the Taitel- Dukler flow regime map. The horizontal stratified flow regime is inside the solid line.

a,c

Figure 6. Plot of jg and jl in the Westinghouse COSI tests (both vertical and horizontal COSI tests) at 7.0MPa against the Taitel- Dukler flow regime map. The horizontal stratified flow regime is inside the solid line.

a,c

Figure 7. Ratio between Estimated Cold Leg Condensation Rate and Measured Value for Validation Cases as a Function of Jet Re Number.

RAI #31: Westinghouse Vertical COSI Downcomer Condensation

WCAP-16996-P/WCAP-16996-NP, Volumes I, II and III, Revision 0,Subsection 17.2.1, "Test Facilities and Tests Description," describes the approach in deriving the Westinghouse vertical COSI cold leg condensation data used to develop the correlation for SI jet condensation in the FSLOCA methodology. It explains that "the COSI experimental data report only gives boiler power and heat loss for the entire test loop." The boiler power was measured and the integral heat loss from the test section, boiler, and pipelines to the environment was estimated. The net total condensation heat transfer rates in the tests were obtained as difference between the boiler power and the heat loss as "steam from the inlet was completely condensed in the Westinghouse COSI tests." To obtain the cold leg condensation test data, the net total condensation rate was split into two parts: (1) condensation rate due to condensation in the cold leg and (2) condensation rate due to condensation in the downcomer. The first part included direct contact condensation on the SI jet in the cold leg and the second part accounted for condensation due to a possible "water fall" in the test section downcomer.

[

]^{a,c} Subsection 17.2.1 Equation (17-2) provides the expressions for the downcomer condensation rate Q_{DC} (in kW) as function of the SI rate m_{SI} (in kg/s):

[ ]^{a,c}
[ ]^{a,c}

Assuming that the identified downcomer water levels were based on the lengths of the corresponding downcomer water falls, the water fall length ratio is assessed as:

[ ]^{a,c}

SI rates were equal in the tests and Equation (17-2) gives the downcomer condensation rate ratio:

[ ]^{a,c}

The downcomer condensation rate ratio is practically equal to the water fall length ratio for the Westinghouse vertical COSI tests used to establish the downcomer condensation rate.

Please provide additional information and clarification with regard to the following items.

(1) Please define the reference elevation used to determine the downcomer levels in [ ]^{a,c} test series. Explain how the downcomer water level was measured and how well was it controlled and maintained in testing.

(2) Please explain if Equation (17-2) was based on the assumption that the condensation rate in the downcomer region was proportional to the length of a free water fall in the steam-filled upper downcomer region. This would allow attributing the difference in the boiler power between the corresponding [ ]^{a,c} tests to difference in the water fall lengths (1.6 m – 0.3 m = 1.3 m) and establishing Equation (17-2).

(3) Please explain if all [ ]^{a,c} runs in each test series were used in establishing Equation (17-2) and present the corresponding test data used.

(4) The expressions in Equation (17-2) were based on information from two Westinghouse [ ]^{a,c} tests that differed only with regard to the downcomer water level. Equation (17-2) correlates the downcomer condensation rate only with the SI

rate and does not take into consideration other important parameters such as SI temperature, pressure, and variations in cold leg and downcomer conditions. If Equation (17-2) was used for all tests listed in WCAP-16996-P/WCAP-16996-NP, Volumes I, II and III, Revision 0, Table 17-2, "Westinghouse Vertical COSI Tests Data," please explain the basis for applying Equation (17-2) under different test conditions and possible implications with regard to the validity of the derived cold leg condensation rates.

Response:

(1) Per WCAP-11767 [1], the reference elevation is the bottom of the test section and the downcomer water level is measured by [

]^{a,c}

(2) The estimation of condensation rate in the downcomer was based on the assumption that the condensation heat transfer rate in the downcomer is [

]^{a,c}

To address this concern, the data reduction process for the COSI tests is revised to more accurately capture the cold leg condensation rate and address the scalability issue. There are two major changes in the revised data reduction process. First, [

]^{a,c} Second, the downcomer condensation rate is evaluated at [ ]^{a,c} using different pairs of tests and the uncertainty of the downcomer condensation rate is applied to the evaluation of the cold leg condensation rate. The process of the data reduction is listed below for the Westinghouse COSI tests.

1. The net condensation heat transfer rate, Q , in the test section (including downcomer) is [ ]^{a,c} (see response to RAI32)
2. The net condensation efficiency is calculated using the following equation

$$\eta_{net} = \frac{Q_{net}}{m_{SI}(h_f - h_{SI})}$$

where Q_{net} is net condensation heat transfer in the test section, m_{SI} is the SI flow rate and h_f and h_{SI} are the enthalpy of saturated water and the SI water (at the test pressure and SI temperature).
3. The net condensation efficiency is [ ]^{a,c} in several runs. The test report did not provide an explanation. In this data reduction process, the net condensation in those cases is [ ]^{a,c}
4. The condensation heat transfer rate in the test section is split into two portions, the condensation in the cold leg and the condensation in the downcomer. The condensation heat transfer rate in the downcomer is evaluated using 3 pairs of tests with only differences being the [

]^{a,c} There are 3 pairs of tests identified for difference pressures, [

]^{a,c} All 5 runs in each pair are used to establish the downcomer condensation efficiency at the particular pressure. The [ ]^{a,c} is the nominal condensation efficiency at the pressure and the maximum and minimum values provide the uncertainty of the downcomer condensation efficiency. The downcomer condensation efficiency and its uncertainty at [

]^{a,c} are calculated as shown in Tables 1 through 3.

5. The net condensation efficiency minus the efficiency caused by downcomer condensation is the cold leg condensation efficiency. [

]^{a,c}

6. The cold leg condensation heat transfer rate is evaluated using the cold leg condensation efficiency and the condensation potential with the formula below.

$$Q_{cond} = \eta_{cond} m_{SI}(h_f - h_{SI})$$

7. [

]^{a,c}

A similar data reduction process is also applied to the Framatome COSI tests using the downcomer condensation efficiency shown in Tables 1 through 3. It is noted that [

]^{a,c} However, the averaged downcomer condensation efficiency in Tables 1 through 3 reduces when the pressure drops from [ ]^{a,c} Thus, the downcomer condensation efficiency of [

]^{a,c} It is also noted that the SI injection rate in the Framatome COSI tests is generally higher than those in the Westinghouse COSI tests. However, the downcomer condensation efficiencies in Tables 1 through 3 [

]^{a,c}

The final results of the cold leg condensation rate and its upper bound and lower bound in the Westinghouse COSI cases and the Framatome COSI cases are collected in Table 4 and Table 5, respectively. Those Tables will replace Table 17-2, Table 17-3 and Table 17-5 in the approved version of WCAP-16996-P.

[

]^{a,c}

It is worthwhile to point out that the condensation heat transfer rate could be interpreted from the measured downcomer temperatures (see Tables 4 and 5) in the tests using the following equation.

$$Q_{net} = m_{SI}(h_{DC} - h_{SI})$$

[

] [a,c]

In summary, the approach to evaluate the condensation rate in the downcomer is revised to better capture the condensation heat transfer rate in the cold leg of COSI facility and to quantify the uncertainties of the condensation heat transfer rate. The revised Westinghouse COSI and Framatome COSI data are shown in Table 4 and Table 5, respectively.

(3) In current submittal of WCAP-16996-P, all the 5 runs in the pair of [ ]^{a,c} tests were utilized to establish the condensation rate in the downcomer [ ]^{a,c} In the revised data reduction process in the response to question (2), all the 5 runs in the pairs of [ ]^{a,c} are utilized to establish the nominal downcomer condensation efficiency and its uncertainty at three different pressures.

4) When the condensation rate in the downcomer was revisited, the influence of [ ]^{a,c} were recognized. Among the parameters, [ ]^{a,c} are primary. Regarding the SI temperature, [ ]^{a,c} In the Framatome COSI tests, [ ]^{a,c} However, the high downcomer water level in the Framatome COSI tests significantly reduced the magnitude of the downcomer condensation rate such that the influence of [ ]^{a,c} Other parameters, such as [ ]^{a,c} are judged as the secondary effect for the evaluation of the downcomer condensation rate.

Reference:

1. WCAP-11767, "COSI SI/Steam Condensation Experiment Analysis," March 1988.

a,c

Figure 1. Comparison between the nominal measured Nusselt number and the Nusselt number predicted from correlation. The measured Nusselt number is reduced from the boiler power.

a,c

Figure 2. Comparison between the nominal measured Nusselt number and the Nusselt number predicted from correlation. The measured Nusselt number is reduced from the downcomer temperature.

Table 1. Evaluation of Downcomer Condensation Efficiency at [ ]^{a,c}

[ ]^{a,c}

Table 2. Evaluation of Downcomer Condensation Efficiency at [ ]^{a,c}

[ ]^{a,c}

Table 3. Evaluation of Downcomer Condensation Efficiency at [ ]^{a,c}

[ ]^{a,c}

Table 4. Westinghouse COSI Test Data

[ ]a,c

Table 4. Westinghouse COSI Test Data (continued)

a,c

Table 4. Westinghouse COSI Test Data (continued)

a,c

Table 5. Framatome COSI Test Data

a,c

RAI #32: Westinghouse Vertical Condensation on Safety Injection Heat Loss

The Westinghouse COSI test data average heat loss and associated uncertainty used to derive the cold leg condensation rates are shown in WCAP-16996-P/WCAP-16996-NP, Volumes I, II and III, Revision 0, Table 17-1, 'Westinghouse COSI Test Data Average Heat Loss and Uncertainty." [

]^{a,c}

Please provide additional information and clarification with regard to the following items.

(1) Please explain how the values for the heat loss uncertainty in Table 17-1 were determined. As the heat loss matched the boiler power, please clarify if the heat loss uncertainties corresponded to the uncertainties in the boiler power. [

]^{a,c}

(2) [

]^{a,c}

(3) Please explain how the boiler power was measured and provide the measurement accuracy.

(4) As seen from Table 17-2 in WCAP-16996-P/WCAP-16996-NP, Volumes I, II and III, Revision 0, Subsection 17.2.1, "Test Facilities and Tests Description," the cold leg condensation rates range between [

]^{a,c}

Considering uncertainties related to heat loss estimates, downcomer condensation rate estimates, and boiler power, please provide estimates for the overall uncertainty of the cold leg condensation data and explain why the data included in Table 17-2 were considered representative and acceptable for the purpose of defining the cold leg condensation correlation.

Response:

(1) Per the COSI test report [1], the heat loss of a test series was measured by [

]^{a,c} There were total 15 heat loss measurements at [ ]^{a,c} in Westinghouse COSI tests. In WCAP-16996-P, the heat loss was assumed to be primarily a function of the system pressure. The heat losses at the same pressure were [

]^{a,c} The results were shown in Table 17-1 of WCAP-16996-P. [

]^{a,c}

In the response to RAI 31, the data reduction process is revised by utilizing [ ]^{a,c}. The approach is consistent to the test procedure and leads to a reduced uncertainty of the heat loss.

(2) The "estimated average heat loss" value is [ ]^{a,c} It is different from the mean value of the uncertainty range. Nevertheless, in the revised data reduction process in the response to RAI 31, the averaged heat loss is not used.

(3) The boiler power is measured by the [ ]^{a,c} Though the detail of the [ ]^{a,c} is not available in WCAP-11767 [1], the uncertainty of the boiler power is given as [ ]^{a,c} The boiler power uncertainty is considered to be a minor factor compared with the uncertainty of the downcomer condensation rate, which is as large as [

]^{a,c}

(4) The experimental uncertainties related to condensation heat transfer rate in the cold leg are [

]^{a,c} As the Westinghouse vertical COSI data were used to generate the correlation and the Westinghouse horizontal COSI data and Framatome COSI data were used for the validation of the cold leg condensation model, the approaches to account for the experimental uncertainty are different.

[

] [a,c]

Reference:

1. WCAP-11767, "COSI SI/Steam Condensation Experiment Analysis," March 1988.

RAI #33: Westinghouse Vertical Condensation on Safety Injection Data and Condensation outside the Jet Region

WCAP-16996-P/WCAP-16996-NP, Volumes I, II and III, Revision 0, Subsection 6.3.6, "Special Model: Cold Leg Condensation Model," clarifies that "the cold leg condensation model assumes that the majority of condensation occurs in a small region near the SI injection port and the condensation outside the mixing zone is negligible." Accordingly, the cold leg SI condensation rates, described in WCAP-16996-P/WCAP-16996-NP, Volumes I, II and III, Revision 0, Subsection 17.2.1"Test Facilities and Tests Description," and presented in Table 17-2, "Westinghouse Vertical COSI Tests Data," were derived as integral condensation rates accounting for the condensation processes in the entire cold leg test section. The characteristic of the Westinghouse Vertical COSI condensation rates is further exacerbated by the fact that the Westinghouse Vertical COSI cold leg test section was significantly oversized in length in comparison to a typical PWR [ ]^{a,c}

In WCOBRA/TRAC-TF2 calculations, the cold leg condensation model is applied to the [

]^{a,c} Please explain if this can lead to over-prediction of the condensation rate for the entire cold leg region in WCOBRA/TRAC-TF2 PWR LOCA analyses due to condensation in the remaining cold leg cells.

Response:

The length of the cold leg in the Westinghouse COSI facility is over-scaled as discussed in the response to RAI30. The development of the correlation assumes that all the condensation (the net condensation rate after removal of heat losses and downcomer condensation) occurs at the mixing zone.

When the cold leg condensation model is applied to separated effects tests, integral effects tests and PWR LOCA, the special condensation model is [

]^{a,c}. Additionally, the special condensation model is active only [

]^{a,c}

The ROSA separate effects test in the validation matrix features a larger cold leg diameter and a properly scaled cold leg length (see the response to RAI 35). The measured condensation heat transfer rate in the cold leg, the predicted cold leg condensation heat transfer rate in the [ ]^{a,c}, and the condensation heat transfer rate of [ ]^{a,c} in the cold leg are collected in Table 1. The measured condensation heat transfer rates are compared with the predicted condensation heat transfer rates of the entire cold leg in Figure 1. [

]^{a,c}

When the cold leg condensation model is applied to PWR LOCA, in which the cold leg scale is larger than both the ROSA and COSI facility, [
]^{a,c}. To confirm this, the condensation heat transfer rate in the cold leg of Beaver Valley Unit 1 is studied. [

]^{a,c}

Figure 2 compares the cold leg condensation heat transfer rate of [ ]^{a,c} in the cold leg starting at the boil-off stage. The condensation heat transfer caused by the SI injection is shown as the solid line and the condensation heat transfer at the accumulator injection node is the blue dashed line. [

]^{a,c}

The results of ROSA tests and Beaver Valley Unit 1 SBLOCA run show that the flow in the cold leg is mostly horizontal stratified with a low interfacial heat transfer rate. [

]^{a,c}

During the refill and reflood stages of a large break LOCA, the cold leg flow regime could be [
]^{a,c} The interfacial heat transfer rate of the [

]^{a,c} The application of the COSI model to the [
]^{a,c} prediction of cold leg condensation in the validation against the full scale UPTF 8A and UPTF 25A tests as shown in Sections 17.3 and 19.3 of WCAP-16996-P.

In summary, [

]^{a,c}

Table 1. ROSA SB-CL-05 SI Condensation Heat Transfer Rate.

[ ] a,c

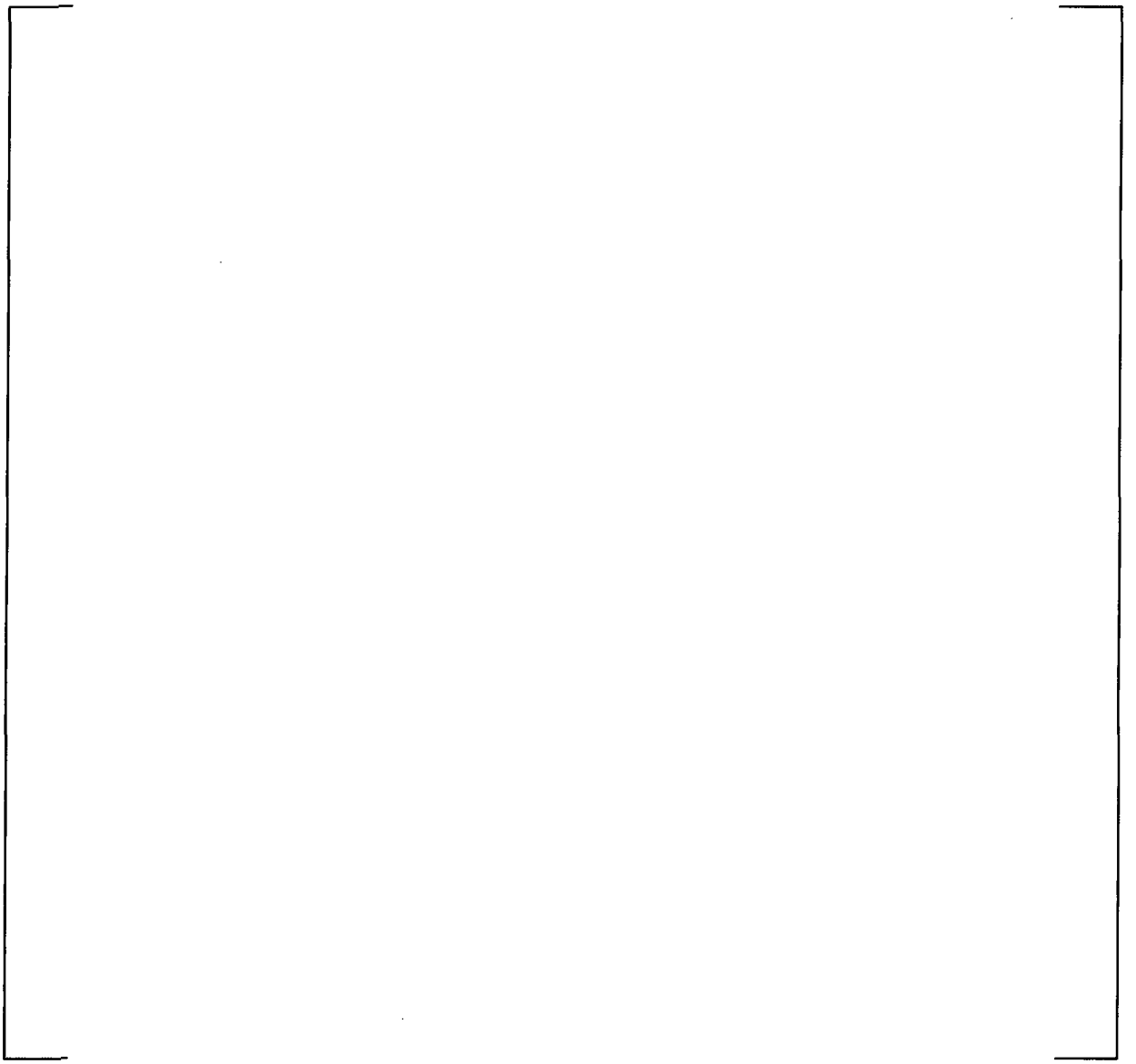

a,c

Figure 1. Comparison between the measured cold leg condensation rate in ROSA and the predicted condensation heat transfer rate of the entire cold leg.

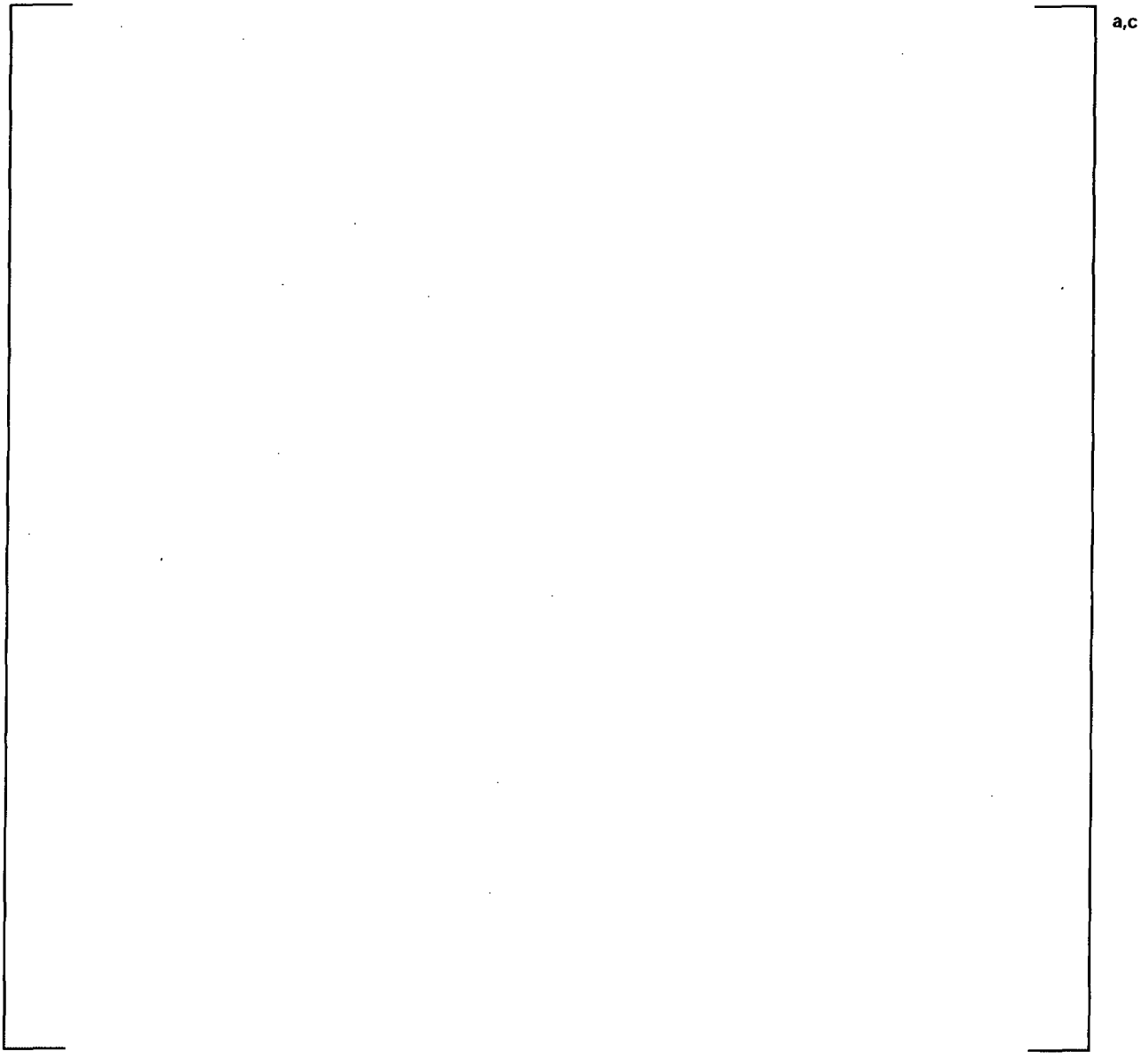

Figure 2. The cold leg condensation heat transfer rate in the [ ]^{a,c} transient.

RAI #34: Westinghouse Vertical Condensation on Safety Injection Data Qualification

With regard to the Westinghouse COSI facility, WCAP-16996-P/WCAP-16996-NP, Volumes I, II and III, Revision 0, Subsection 17.2.1, "Test Facilities and Tests Description," states that "a core series of 15 tests, with 75 individual data, from Westinghouse configuration was conducted." The Westinghouse vertical COSI cold leg condensation rates used to define the empirical correlation for prediction of direct contact condensation on SI water in the cold legs are presented in WCAP-16996-P/WCAP-16996-NP, Volumes I, II and III, Revision 0, Table 17-2, "Westinghouse Vertical COSI Tests Data." The table contains 60 data points. In addition, Figure 6-15 in WCAP-16996-P/WCAP-16996-NP, Volumes I, II and III, Revision 0, presents a comparison between the calculated Nusselt number and the measured Nusselt number for the fitted data points.

Please clarify and address, as needed, the following items related to the set of Westinghouse vertical COSI data, which was utilized to define the SI condensation correlation.

(1) Please explain if all available Westinghouse vertical COSI test runs were assessed and reported as "points" in the second column of WCAP-16996-P/WCAP-16996-NP, Volumes I, II and III, Revision 0, Table 17-2. Clarify if any estimated condensation rates were disregarded and not included as "points" in Table 17-2 and if so please explain the reasons. In addition, please clarify if all data points in Table 17-2 were plotted in Figure 6-15.

(2) Table 17-2 provides only the derived condensation rates and does not include the measured boiler power, estimated downcomer condensation rate, and downcomer level. Please provide an expanded table that includes also these test parameters.

Response:

(1) In Westinghouse COSI tests, there is a total of 75 data points [

]^{a,c}

(2) The measured boiler power and downcomer water level are shown in Table 4 in the response to RAI 31. Table 17-2 will be updated to include the measured boiler power and downcomer water level in the approved version of WCAP-16996-P. The estimated downcomer condensation rate is given in Tables 1 through 3 in the response to RAI 31 and was used to calculate the nominal lower bound and upper bound Qcond values in Table 4.

RAI #35: Scale Impact on Cold Leg Condensation

WCAP-16996-P/WCAP-16996-NP, Volumes I, II and III, Revision 0, Subsection 6.3.6, "Special Model: Cold Leg Condensation Model," and Subsection 17.2.1, "Test Facilities and Tests Description," explain that the Westinghouse horizontal injection COSI dataset, Framatome COSI dataset and ROSA-IV large scale test facility (LSTF) Test SB-CL-05 SI condensation separate effects test dataset were used "to independently perform the validation" of the cold leg condensation model.

The cold leg diameter of the Westinghouse and Framatome test sections was [ ]^{a,c} The length of the Framatome cold leg test section was only [ ]^{a,c} from the inlet to the downcomer compared with [ ]^{a,c} in the Westinghouse test section. The Westinghouse horizontal COSI test section had an SI line attached at [ ]^{a,c} longitudinal angles with an increased diameter of [ ]^{a,c}. The Framatome COSI test section had an SI line with a diameter of [ ]^{a,c} and was oriented at [ ]^{a,c} azimuthal angle and [ ]^{a,c} longitudinal angles. The downcomer water level in the Framatome COSI tests was at [ ]^{a,c} and the downcomer condensation rate was evaluated using Equation (17-2). A subset of qualified Framatome COSI test runs that had zero break flow vented out of the test facility exiting the cold leg test section were used in the validation process are shown in the Table 17-5.

The LSTF was a 1/48 volumetrically scaled model of a Westinghouse-type 3423 MWt four loop PWR. The cold legs were sized to preserve the volumetric ratio and the pipe length-to-square root of diameter, $L/(D)^{0.5}$, ratio for the reference PWR. The table below summarizes major geometric parameters for the test facility.

Table: Major Geometry Parameters for LSTF ROSA-IV

Parameter	LSTF	Prototype	Length Ratio
Cold leg diameter (in)	8.15	27.5	3.4
SI line diameter (in)	3.44	5.20	1.5
Cold leg pipe length (ft)	12.1	22.9	1.9
Azimuthal angle (deg)	90°	90°/45°	-
Longitudinal angle (deg)	45°	90°	-

For the purposes of validating the cold leg condensation model in the FSLOCA methodology, a simple modeling approach using a TEE component as shown in Figure 17-9, was applied to both the Westinghouse horizontal COSI and Framatome COSI test facilities. The noding diagram for the ROSA-IV SB-CL-05 safety injection tests was similar to that of the Westinghouse vertical COSI facility. A separate noding diagram, shown in Figure 17-10, was used for Framatome counter-current COSI tests.

Please clarify the following items related to the validation of the cold leg condensation model in the FSLOCA methodology that was derived from Westinghouse vertical COSI test data.

(1) Both the Westinghouse and Framatome COSI experiments were performed with the same cold leg diameter of [ ]^{a,c} and with the same downcomer geometry. Key geometry differences involved only the orientation and diameter of the SI injection line. The calculation for the heat loss, downcomer condensation, and upper and lower bound of the cold leg condensation rates for the Framatome tests followed the same procedure that used for the Westinghouse COSI data reduction. Please explain how the Westinghouse horizontal injection COSI dataset and the Framatome COSI dataset contribute to the validation of the FSLOCA methodology cold leg condensation model. Provide the resolution

of identified open items pertaining to the Westinghouse vertical COSI tests that are also applicable to the Westinghouse horizontal injection COSI dataset and the Framatome COSI dataset.

(2) ROSA-IV LSTF Test SB-CL-05 was used as a separate effects test for cold leg SI condensation by modeling only the cold leg and SI injection portion in ROSA-IV and using test measurements of instantaneous flow conditions in the cold leg at four selected instances [ ]^{a,c} Please explain which of the flow parameters in Table 17-7, "ROSA SB-CL-05 SI Condensation Test Data for separate effects tests (SETs)," were measured and how the provided experimental values were established and qualified. For example, test measurements can exhibit noticeable oscillations in time. For all remaining parameters in Table 17-7, if any, please provide the expressions used for their calculation.

(3) WCAP-16996-P/WCAP-16996-NP, Volumes I, II and III, Revision 0, Subsection 17.2.2, "Description of WCOBRA/TRAC-TF2 Models," explains that in the cold leg condensation model validation studies based on the Westinghouse horizontal COSI test facility, Framatome COSI test facility, and ROSA-IV LSTF, a simple modeling approach with a TEE component was applied to simulate only "the scaled part of the cold leg" with the side TEE junction representing the injection port. Please explain how "the scaled part of the cold leg" was determined in the assessment studies and show that the applied scaling has no impact on the assessment results.

(4) The comparison between the calculated condensation rates and the experimentally derived rates for LSTF ROSA-IV SB-CL-05 cold leg condensation test, shown in Figure 17-13, indicates that WCOBRA/TRAC-TF2 under-predicted all four rates. WCAP-16996-P/WCAP-16996-NP, Volumes I, II and III, Revision 0, Section 17, "Cold Leg Condensation: COSI Experiments, ROSA-IV SB-CL-05 Experiment, and UPTF-8A Experiment," does not provide direct comparison of WCOBRA/TRAC-TF2 predictions for the SI condensation rate against test data from test facilities other than COSI and LSTF. Please demonstrate that the WCOBRA/TRAC-TF2 cold leg condensation model will not inherently and systematically over-predict the cold leg condensation rate in PWR LOCA analyses if such a model is based on indirect measurements in a single scaled test facility with regard to PWR cold leg geometry.

Response:

(1) Both the Westinghouse horizontal COSI tests and the Framatome COSI tests are part of validation matrix for the cold leg condensation model. The only difference between the Westinghouse horizontal COSI tests and the vertical COSI tests is the SI line diameter and the injection angle. Other parameters, such as the system pressure, SI flow rate and boiler power are similar in both tests. It was discussed in the response to RAI 30 that the diameter of SI line is [

]^{a,c}

Framatome COSI shared the same testing facility with Westinghouse COSI but with a shorter cold leg test section as shown in Figure 17-5 of WCAP-16996-P. The shorter cold leg is more appropriate from a scaling standpoint. The scaling effect of the cold leg diameter in the response to RAI 30 is applicable to the Framatome COSI test facility. [

]^{a,c} in Westinghouse COSI shown in Table 1 of the response to RAI 30, which is [

]^{a,c}

[

]^{a,c}

Since the cold leg diameter is the same for both the Westinghouse COSI tests and the Framatome COSI tests, the discussion on the cold leg diameter effect in the response to RAI 30 is applicable to the Framatome COSI test.

[

]^{a,c}

a,c

Figure 1. Plot of jg and jl in the Framatome COSI tests at 7.0 MPa against the Taitel Dukler flow regime map. The horizontal stratified flow regime is inside the solid line.

a,c

Figure 2. Plot of jg and jl in the Framatome COSI tests at 2.0 MPa against the Taitel Dukler flow regime map. The horizontal stratified flow regime is inside the solid line.

(2) The ROSA SB-CL-05 experiment is an integral effects test featuring high head safety injection toward the cold leg. Unlike the COSI experiment, there was no steady state in the cold leg during the ROSA test. However, it is found that the cold leg flow condition in the boil off stage of SB-CL-05 is stable and the transient is slow. [

]^{a,c}

The ROSA SB-CL-05 data reduction process included the use of raw data, establishing data points and converting test data to condensation heat transfer rates. First, the measured pressure transient of the experiment was used. [

]^{a,c}

[

]^{a,c}

a,c

Figure 3. Pressurizer pressure transient in ROSA SB-CL-05 (Figs. 5.7 and 5.8 in Reference [2]).

a,c

Figure 4. Measured fluid temperature in the cold leg and SI temperature. (Reference [2]).

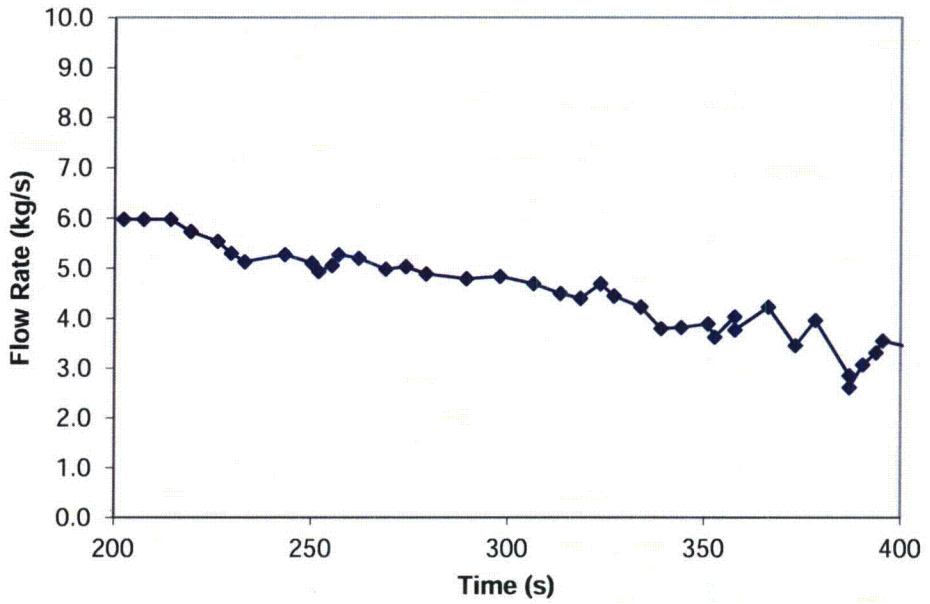

Figure 5. Measured Intact loop (Loop A) steam flow rate in ROSA SB-CL-05. (Reference [2]).

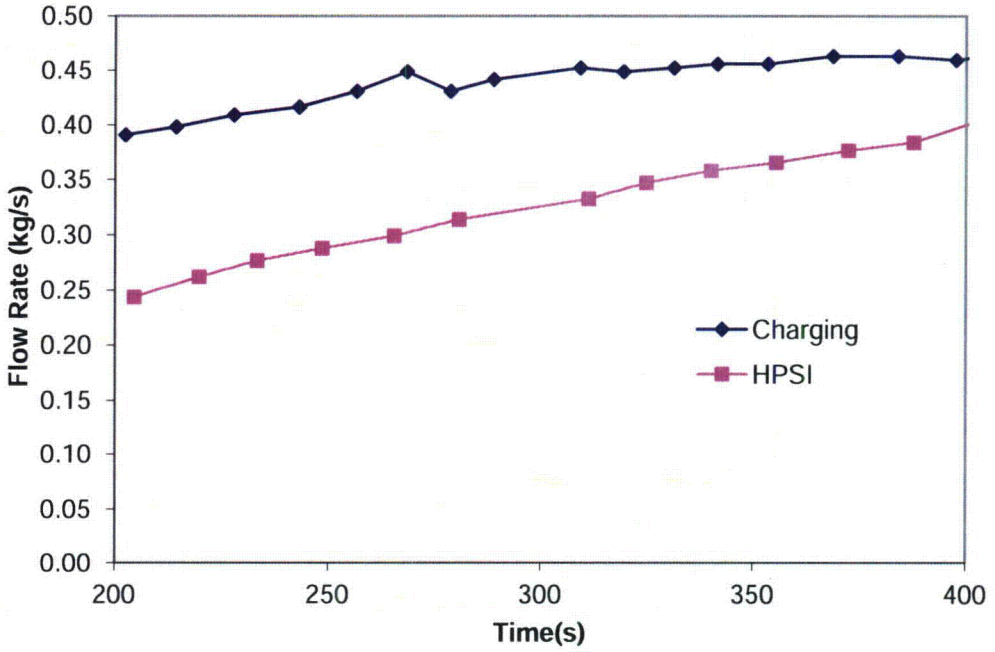

Figure 6. Measured Intact loop (Loop A) ECC flow rates in ROSA SB-CL-05. (Reference [2]).

(3) It is clarified that, in the validation cases, both the Westinghouse horizontal COSI tests and the Framatome COSI tests were simulated with [

]^{a,c} In the response to RAI 30, it was shown that the extra length of the cold leg in the COSI facility is a secondary effect on the cold leg condensation rate though a bias was introduced. The results of ROSA prediction presented in the response to RAI 33 indicates that the total condensation rate of the properly scaled ROSA cold leg is [

]^{a,c} The Beaver Valley Unit 1 cold leg condensation prediction also shows that [

]^{a,c}

(4) The condensation heat transfer rates were compared to the Westinghouse COSI tests, the Framatome COSI tests, and the ROSA SB-CL-05 tests to demonstrate the performance of the cold leg condensation model. However, the data reduction to obtain condensation heat transfer rate followed different approaches. [

]^{a,c} A detailed data reduction process has been provided in the response to question (2).

The main reason the condensation heat transfer rate comparison was not provided for the assessment of UPTF 8A and UPTF 25A is that, unlike SBLOCA tests of COSI and ROSA SB-CL-05, the temperature measurements in LBLOCA tests such as UPTF 8A showed excessive oscillations. The oscillations impact the data reduction process when converting the cold leg temperature to the condensation heat transfer rate. It is more appropriate to compare the measured cold leg temperature and the predicted cold leg temperature to assess the condensation prediction in LBLOCA cases. [

]^{a,c} If the condensation heat transfer rate is [

]^{a,c} Section 17.3 in WCAP-16996-P shows the water temperature at the outlet of the cold leg was [

]^{a,c}

However, the condensation effect can be indirectly compared with the steam condensation rate. The predicted steam condensation rate in the UPTF 8A loop 2 cold leg is compared with the estimated steam condensation rate by MPR [3]. The steam condensation rate is defined as the steam flow rate difference between the inlet and the outlet of cold leg. Figure 7 shows the predicted values [ ]^{a,c} The steam condensation rate is [

]^{a,c} Those behaviors are consistent with the cold leg temperature prediction in Section 19.3.8 of WCAP-16996-P.

a,c

Figure 7. Comparison between the predicted steam condensation rate and the measured steam condensation rate in UPTF 8A experiment. The ECC flow rate points (100kg/s to 600kg/s) correspond to UPTF 8A stages 6 through 1.

References:

1. WCAP-11767, "COSI SI/Steam Condensation Experiment Analysis," March 1988.
2. JAERI-memo 61-056, ROSA-IV/LSTF 5% Cold Leg Break LOCA Experiment Data Report: Run SB-CL-05, March 20, 1986.
3. MPR-1208, Summary of Results from the UPTF Cold Leg Flow Regime Separate Effects Tests, Comparison to Previous Scaled Tests, and Application to U.S. Pressurized Water Reactors, MPR Associates, 1992.